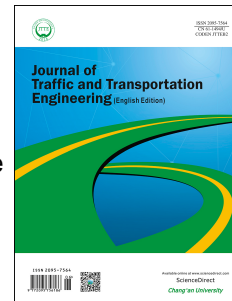


Journal Pre-proof

Development of port fuel injected methanol (M85)-fuelled two-wheeler for sustainable transport

Tushar Agarwal, Akhilendra Pratap Singh, Avinash Kumar Agarwal



PII: S2095-7564(20)30062-3

DOI: <https://doi.org/10.1016/j.jtte.2020.04.003>

Reference: JTTE 300

To appear in: *Journal of Traffic and Transportation Engineering (English Edition)*

Received Date: 9 March 2020

Revised Date: 24 April 2020

Accepted Date: 25 April 2020

Please cite this article as: Agarwal, T., Singh, A.P., Agarwal, A.K., Development of port fuel injected methanol (M85)-fuelled two-wheeler for sustainable transport, *Journal of Traffic and Transportation Engineering (English Edition)*, <https://doi.org/10.1016/j.jtte.2020.04.003>.

This is a PDF file of an article that has undergone enhancements after acceptance, such as the addition of a cover page and metadata, and formatting for readability, but it is not yet the definitive version of record. This version will undergo additional copyediting, typesetting and review before it is published in its final form, but we are providing this version to give early visibility of the article. Please note that, during the production process, errors may be discovered which could affect the content, and all legal disclaimers that apply to the journal pertain.

© 2020 Periodical Offices of Chang  an University. Publishing services by Elsevier B.V. on behalf of Owner.

1 **Original Research Paper**

2
3 **Development of port fuel injected methanol**

4 **(M85)-fuelled two-wheeler for sustainable transport**

5 **Tushar Agarwal, Akhilendra Pratap Singh, Avinash Kumar Agarwal***

6
7 *Engine Research Laboratory, Department of Mechanical Engineering, Indian Institute of Technology*
8 *Kanpur, Kanpur 208016, India*

9
10 **Highlights**

- 11 • A functional M85-fuelled two-wheeler prototype was developed.
12 • ECU recalibration for methanol fueling was done.
13 • Comparison of gasoline-fuelled motorcycle vis-à-vis M85-fuelled motorcycle.
14 • M85-fuelled motorcycle exhibited improved vehicle performance.
15 • M85 is a sustainable fuel for two-wheeler applications.

16
17 **Abstract**

18 Due to increasingly stringent environmental pollution norms, there is a need for alternate
19 combustion techniques and alternate fuels to keep up with changing trends. One of the
20 viable solutions for India is the adaptation of methanol as a fuel for automotive sector.
21 Therefore, in this study a functional two-wheeler prototype was developed, which uses
22 M85 (85% v/v methanol and 15% v/v gasoline) in an electronic control unit (ECU)
23 controlled port fuel injected (PFI) engine. This study included comparative investigations of
24 simulated on-road two-wheeler performance on chassis dynamometer using a
25 gasoline-fuelled motorcycle with stock ECU vis-à-vis M85-fuelled motorcycle using
26 recalibrated ECU. ECU recalibration exhibited that M85-fuelled vehicle was operated at

27 relatively more advanced spark timing compared to baseline gasoline-fuelled vehicle.
28 Performance results showed that M85-fuelled motorcycle produced relatively higher
29 engine power and higher maximum vehicle speed compared to gasoline-fuelled
30 motorcycle. Relatively superior acceleration characteristics (especially at higher speeds)
31 of M85-fuelled motorcycle was another important finding of this study, indicating that M85
32 provided superior throttle response compared to gasoline. Comparative analysis of raw
33 tailpipe emissions showed that modified M85-fuelled motorcycle emitted relatively higher
34 hydrocarbon (HC), carbon monoxide (CO) and oxides of nitrogen (NO_x) emissions
35 compared to stock gasoline-fuelled motorcycle. However, these emissions can be
36 controlled by using adaptation of suitable after-treatment systems.

37

38 **Keywords:**

39 Methanol; Electronic control unit (ECU); Electronic fuel injection (EFI); ECU calibration; Engine
40 performance; Emission.

41

42

43 * Corresponding author. Tel.: + 91 512 259 7982; fax: + 91 512 259 7408.

44 E-mail addresses: tushki96@gmail.com (T. Agarwal), akhilendrapdf@gmail.com (A.P. Singh),
45 akag@iitk.ac.in (A.K. Agarwal).

46

1 Introduction

There has been a rapid increase in consumption of fossil fuels since last century and hence equivalents rise in their depletion rate. There are a number of factors such as increase in energy consumption per capita in developing countries, increased industrial investments, etc., which have led to many folds increase in fossil fuel consumption rate (Nesamani et al., 2017; Smil, 2017). Since reserves of these fossil fuels on earth are rather limited and they have very large carbon footprint therefore, there is a need to explore other alternate fuels and energy resources. This motivated the researchers globally to develop non-conventional, low carbon, renewable fuels, which can keep up with the pace of development in a sustainable manner. In search of these alternatives, a large number of potential fuels such as SVO (No, 2017; Patel et al., 2019), biodiesel (Geng et al., 2018; Singh et al., 2017a, b), hydrogen (Pal and Agarwal, 2015; Singh et al., 2017a, b), alcohols (Agarwal et al., 2014, 2019; Singh et al., 2015), etc., have been extensively explored, however, each fuel has their own advantages and disadvantages (Agarwal, 2007; Chen et al., 2018). Among these alternative fuels, alcohols were found the most suitable alternative fuel for a variety of vehicles including two-wheelers, light-duty vehicles (LDVs) and heavy-duty vehicles (HDVs).

Primary alcohols such as methanol, ethanol and butanol constitute a potential class of alternative fuels, offering several benefits over petroleum derivatives, specifically gasoline. Methanol is a primary alcohol, which has proved its potential as an alternative fuel for internal combustion (IC) engines. Methanol has several fuel properties that are superior to baseline gasoline that makes it fit for use in IC engines (Verhelst et al., 2019). Methanol has higher latent heat of vaporization (LHV) and a lower flame temperature than gasoline, which leads to lower heat losses through the engine, hence a superior thermal efficiency (Agarwal et al., 2019). This also means a cooler intake process that increases the volumetric efficiency of the engine. Methanol has a lower boiling point, higher oxygen content (50% w/w) and a greater laminar flame propagation speed than gasoline (Chen et al., 2020; Liao et al., 2005; Wei et al., 2008), which helps in reduction of toxic emissions. Methanol is a liquid fuel, which has handling, storage and transportation practices similar to gasoline. Methanol can be produced from a variety of resources such as coal, natural gas and biomass in an economically viable manner. Due to these features, methanol has been reported as more suitable alternative fuel compared to other primary alcohols such as ethanol (Anderson et al., 2010; Nicholas, 2003; Yao et al., 2018).

To investigate the effects of methanol on engine combustion, performance and emission characteristics, many researchers have carried out engine experiments as well as modelling studies. Wei et al. (2008) conducted engine experiments to investigate the effects of methanol-gasoline blends on a three-cylinder, electronic port fuel injection, four-stroke spark ignition (SI) engine. They reported an increase in brake thermal efficiency (BTE) with increasing methanol proportion in the test blend. The peak in-cylinder pressure (P_{max}) increased by 17.6% in case of M85 (85% v/v methanol and 15% v/v gasoline) compared to gasoline with an advancement of 4-5 crank angle degree (CAD), and the ignition delay and combustion duration were shortened. In addition, carbon monoxide (CO) emission decreased by 25% and oxides of nitrogen (NO_x) emission decreased by 80% for M85 with respect to baseline gasoline. Siwale et al. (2014) studied the performance, emission and combustion characteristics of methanol-gasoline blends in a multi-cylinder, naturally aspirated SI engine. They compared the combustion and performance characteristics of M0 (pure gasoline), M20 (20% v/v methanol and 80% v/v gasoline), M70 (70% v/v methanol and 30% v/v gasoline) and M53B17 (53% v/v methanol, 17% v/v n-butanol and 30% v/v gasoline). They reported that M70 showed the highest BTE among different test fuels. Use of methanol is not limited in only SI engines because many researchers investigated the effect of methanol blending in diesel engines. Dhaliwal et al. (2000) investigated the emission characteristics of methanol and reported that M100 emitted lower NO_x and particulate matter (PM) compared to baseline diesel, whereas a mixed trend was observed for hydrocarbon (HC) and CO. Agarwal et al. (2019) also carried out engine experiment using different blends of methanol and mineral diesel in a genset engine and reported that addition of methanol in mineral diesel resulted in superior combustion and emission characteristics compared to baseline mineral diesel. They observed a significant reduction in PM and suggested that methanol-diesel blends are capable to resolve NO_x -PM trade-off up to medium engine loads. These investigations showed the potential of methanol for the adaptation in automotive sector. However, adaptation of alternative fuels only in four-wheelers sector will not be enough to resolve the issues of road transport in developing countries like India, China, etc., as two-wheelers play an important role in such countries. In India, two-wheelers dominate over four-wheelers in which most of them use gasoline. Therefore, serious research efforts are required to develop clean and efficient two-wheeler engine technologies, which should be capable of alternative fuel utilization.

Over the years, there have been many technological advances in the two-wheeler powertrain.

Researchers have come up with various strategies for improving performance, emissions and combustion characteristics of two-wheelers. Adopting a new technology developed for cars in two-wheelers is not easy because of several constraints, among which space available is an important one. For developing a new technology, additional components can be easily fitted in four-wheelers, however, in two-wheelers, fitment of additional components is a challenging task. Often, it is not even possible to adopt a four-wheeler technology in compact two-wheelers. For a very long time, carbureted two-stroke engines dominated the two-wheeler segment. Use of alcohols in carbureted SI engines either as 100% methanol or by blending it with gasoline has been explored by numerous researchers. Paramasivam et al. (2018, 2019, 2020) investigated the emission characteristics of two-wheeler fuelled with different gasoline-ethanol blends vis-à-vis baseline gasoline. They reported that the addition of ethanol in gasoline resulted in lower HC, CO and NO_x emissions compared to baseline gasoline, however, they resulted in higher concentration of unregulated species such as carbonyls, saturated hydrocarbons, aromatics, etc. Similar results were also reported by Costagliola et al. (2016) and Yang et al. (2012), who carried out experiments using gasoline-alcohol blends in scooter and motorcycle, respectively. Li et al. (2015) conducted experiments on a carbureted motorcycle engines of 110 cc, 125 cc and 150 cc using M15 (15% v/v methanol and 85% v/v gasoline). All motorcycles were tested for both M15 and gasoline, and no modifications were made to the fuelling system. They used the urban driving cycle (UDC) for their testing and similar performance from both test fuels. Emission characterization showed a significant reduction in HC, CO and NO_x concentrations emitted from M15-fuelled engines. Similar to ethanol, methanol blending with gasoline also resulted in higher concentration of unregulated species.

Latey et al. (2005) conducted experiments in a single cylinder carbureted two-wheeler engine in which methanol (M20) was injected using port fuel injection (PFI) technique and compared its performance with electronic fuel injection (EFI) system. They reported that operating engine hardware of the EFI system produced higher power and provides superior fuel economy compared to the carburetor. EFI system provided significantly higher power output compared to carbureted engine of same capacity and resulted in better BTE. Gong et al. (2011) investigated the effects of addition of liquefied petroleum gas (LPG) to methanol on the engine firing behavior and unregulated emissions. They conducted the experiments in an electronically controlled, 125 cc SI engine with a compression ratio of 10.55. They reported that mixing of LPG with methanol improved the cold starting performance

of two-wheelers. Although methanol utilization in engines has many advantages such as performance and emission improvement along with economic benefits, however, there are few challenges, which limit its application in the production grade engines/vehicles. Corrosiveness of methanol is one such critical issue, which harms few soft engine components made of plastic, rubber seals and metallic ones in the fuel supply system. Therefore, it is necessary that precautions should be taken during the engine operation fuelled with methanol (Iliev, 2018).

Many researchers have successfully demonstrated methanol adaption in traditional engines along with significant improvements in performance and emissions. Most research on two-wheeler engines using methanol has focused on carbureted engines. In few studies, PFI system has been adapted for methanol utilization, however this technique was also limited up to low fraction of methanol (below 40%). Therefore, the development of methanol-fuelled two-wheelers remains a promising field of research, where technology for utilization of higher fractions of methanol can be developed. This study focused on the development of an EFI system based two-wheeler using higher fractions of methanol (M85). This was achieved by recalibrating the ECU by developing ECU calibration maps for M85. Optimization of engine operating parameters for M85 was another novel aspect of this study, which exhibited acceptable on-road drivability and performance, similar to or better than the base gasoline vehicle. To verify the final M85 ECU maps, modified M85-fuelled motorcycle was tested against the stock gasoline-fuelled motorcycle using industry vehicle standard performance parameters. A comparative analysis of performance and emission characteristics of modified M85-fuelled two-wheeler vis-à-vis stock ECU based gasoline-fuelled two-wheeler was another important aspect of this study. Overall, this study provided an idea about the journey of a successful M85-fuelled two-wheeler prototype vehicle development and its concept verification, which has not been reported in previous studies.

2 Materials and methods

The experimental methodology followed to perform this experimental investigation is shown in Fig. 1.

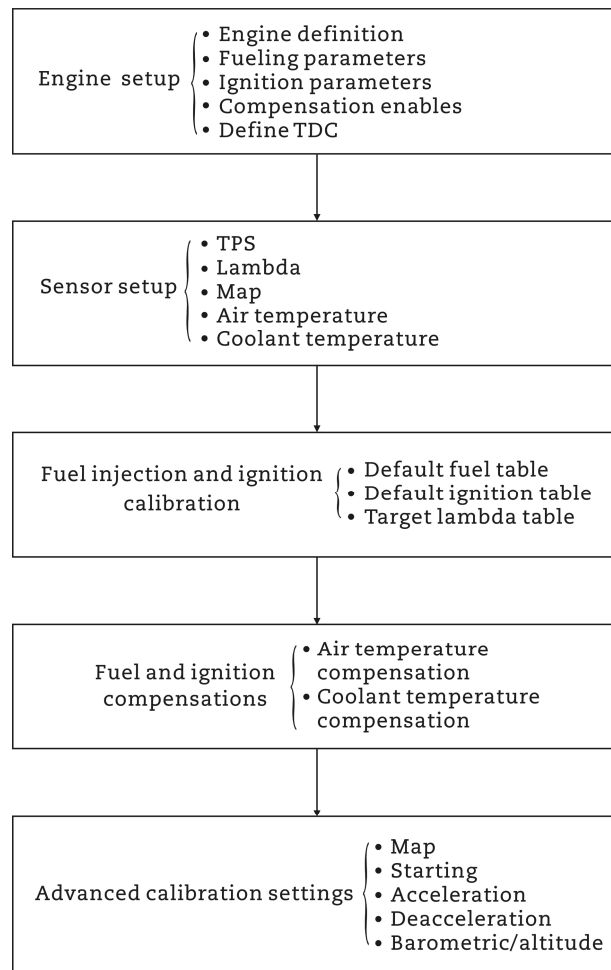


Fig. 1 Block diagram of experimental methodology.

Detailed explanations of these steps have been discussed in our previous publication (Agarwal et al., 2020). Important steps involved in this study are given in appendix. In this study, experiments were carried out using two different experimental setups namely engine experimental setup and vehicle test setup. Engine experiments were performed 500 cc engine (make: Royal Enfield; model: Classic 500) using M85. Detailed technical specifications of the test engine are given in Table 1.

Table 1 Specifications of test engine.

Parameter	Value
Make	Royal Enfield
Model	Classic desert storm 500 cc (BS IV model)
Displacement per cylinder	499 cc
Injection type	Electronic port fuel injection
Number of cylinders	1
Bore/stroke	84 mm/90 mm
Valves per cylinder	2 (1 inlet, 1 exhaust)

Stock power output	20.28 kW at 5250 rpm
Stock peak torque	41.3 N·m at 4000 rpm
Compression ratio	8.5 : 1
Cooling type	Air cooled
Lubrication	Dry sump positive plunger type
Electric control unit (ECU)	Keihin 571056/a
Fuel injection pressure	3 bar
Crank position sensor type	Variable reluctance type

The test engine was mounted on a three degree of freedom cast iron base and coupled to an eddy current engine dynamometer via chain-sprocket arrangement. Experiment setup for engine dynamometer testing and calibration is shown in Fig. 2.

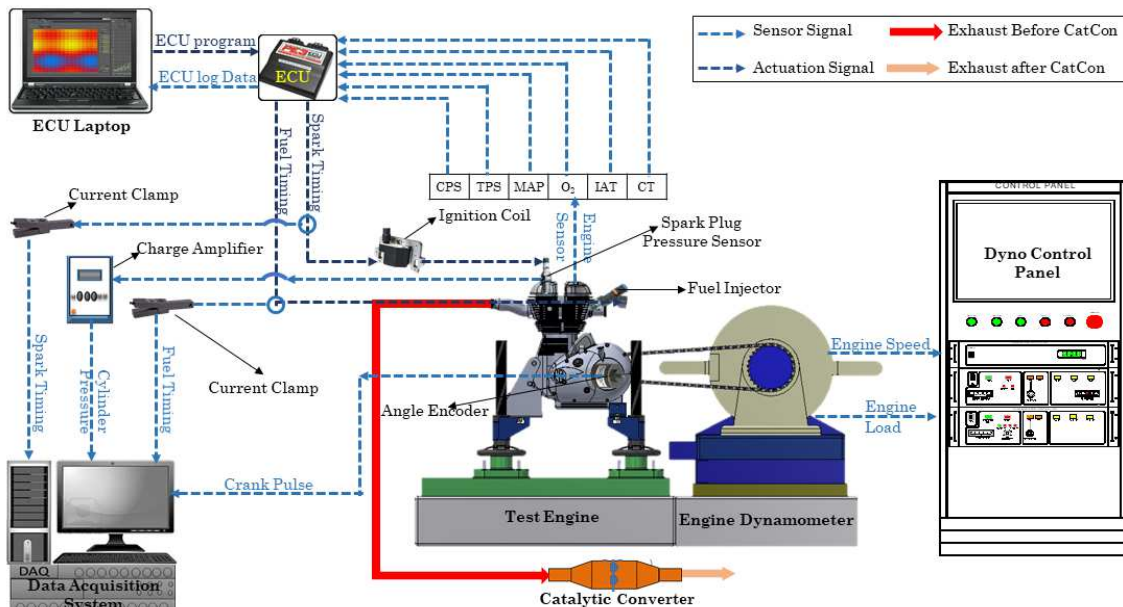


Fig. 2 Schematic of engine dynamometer test setup.

The engine has a single exhaust valve and a single intake valve engine with dry sump positive plunger type lubrication. For the experiments, electronic fuel injection strategy was used, which was controlled by an ECU (make: Keihin; model: 571056/a). The flywheel or crankshaft of the engine was attached to the resistance/brake unit of the dynamometer (make: Dynalec Controls India; Model: ECB-50-200) for simulating the road load driving conditions. The engine was pre-equipped with various sensor such as crank position sensor, throttle position sensor, manifold air pressure sensor, ambient air temperature sensor and engine temperature sensor. The data from these sensors were used by the

stock ECU to adjust the fuel injection duration and spark timings by actuating the fuel injector and ignition coil accordingly. To reverse engineer the stock ECU gasoline maps, a combustion analyzer (make: Hi-Technique, model: Synergy) was used to measure various engine parameters such as engine speed, spark timing, fuel injector duration and throttle opening. To measure the spark timing and fuel injection duration, spark plug and fuel injector input cables coming from the ECU were tapped using current clamps (make: Chauvin Aenoux; model: E3N). To recalibrate the ECU for M85, stock ECU was replaced with an open ECU (make: Power Electronics; model: PE3 SP000). No change was in the engine wiring harness though. The open ECU was controlled using a laptop connected to the ECU via an Ethernet cable. ECU measured the engine speed, throttle opening, intake manifold pressure, lambda and engine temperature using suitable sensors (Fig. 3). Based on these values, it calculates the injector open time and the spark timing, and accordingly actuated the ignition coil and fuel injector.

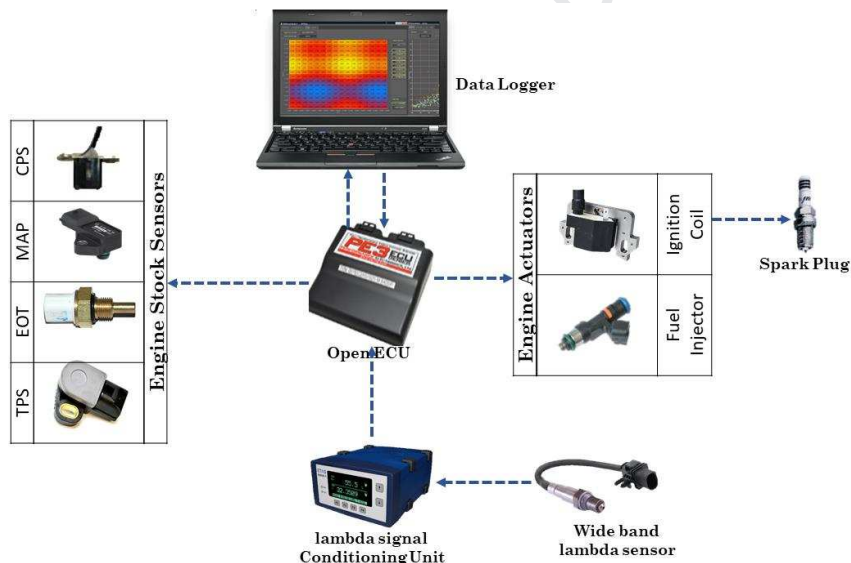


Fig. 3 Schematic for ECU calibration setup.

Vehicle tests were performed on another setup equipped with chassis dynamometer. In chassis dynamometer, the entire vehicle was mounted on the dynamometer, whose rollers apply resistance to the driving wheel of the vehicle. The driving test was conducted on the chassis roller, which is a high inertia drum connected to AC regenerative motor. Schematic of experimental setup is shown in Fig. 4.

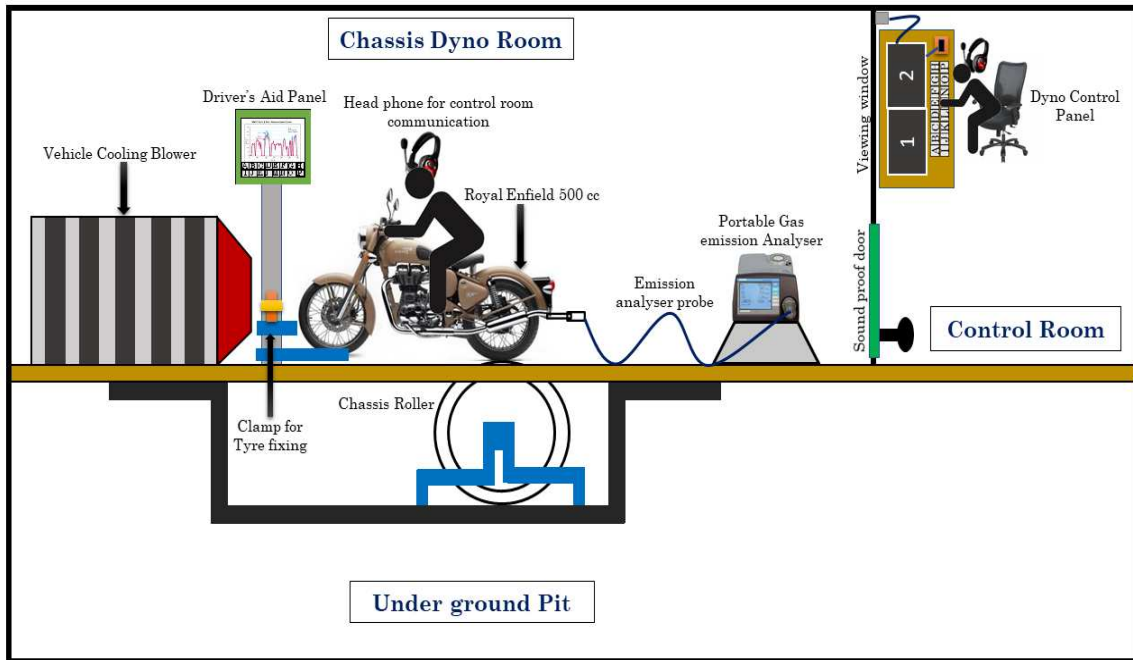


Fig. 4 Schematic of chassis dynamometer test setup.

This setup was divided into two sections as dynamometer room and control room. Dynamometer room consisted of a checkered base plate covering the underground pit. A small portion of classis roller popped out of this checkered base plate, on which the rear/driving wheel of two-wheeler rest. Front wheel of the motorcycle was pneumatically clamped to the test bed. The motorcycle was securely attached to the test bed using restraining cables at multiple locations for safety. Dynamometer room was equipped with a driver aid panel, which displayed important test parameters such as vehicle speed, drive gear and test cycle graph. This information was used by the rider to accordingly control the throttle, brake and drive gear of the motorcycle. To cool the motorcycle and to simulate air resistance to the vehicle during actual road driving condition, a three phase heavy-duty blower with variable frequency drive was used. The speed of air coming from the blower was synchronized with the motorcycle speed for accurately simulating the road driving conditions. The operator feeds testing cycles into dynamometer control panel and logs the test results to the computer. The underground pit housed an AC regenerative motor for simulating the vehicle load conditions. This regenerative motor was connected to chassis roller, on which the driving wheel of motorcycle rests. All the wirings of the cooling blower, driver aid panel and AC regenerative motor were routed through underground trenches such that the checkered base plate seats are mounted flush with the dynamometer room floor. In order to measure the pollutants from the engine, a raw exhaust gas emission analyzer (make: Horiba; model MEXA 584L) was used in this study. Raw exhaust gasemission analyzer was capable of measuring

different gaseous exhaust species such as CO, HC, NO_x, and CO₂. Other technical details of the gaseous emission analyser are given in Table 2.

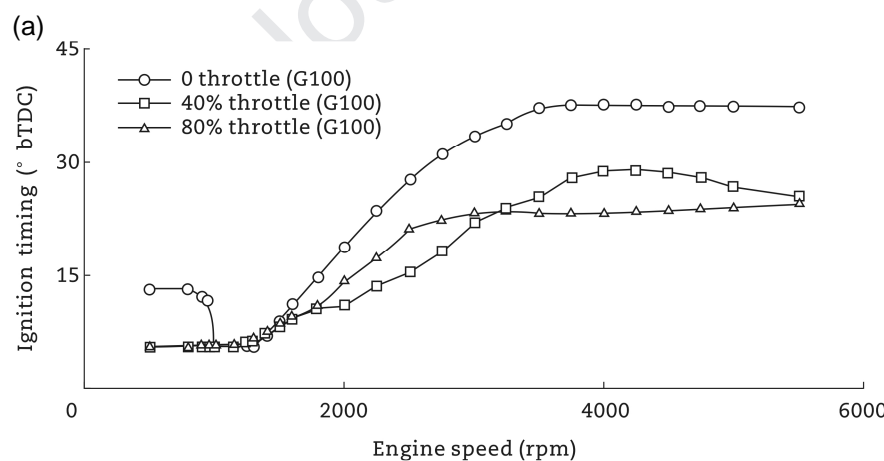
Table 2 Details of exhaust gas emission analyser.

Species	Measurement principle	Range	Repeatability
CO	Non-dispersive infrared (NDIR)	0 to 10%	0.01%
HC	Non-dispersive infrared (NDIR)	0 ppm to 20000 ppm	3.3 ppm
CO ₂	Non-dispersive infrared (NDIR)	0 to 20%	0.17%
NO _x	NO sensor	0 ppm to 5000 ppm	5.0 ppm

3 Results and discussion

3.1 Comparison of gasoline ignition map vis-à-vis M85 ignition map

In Fig.5, base gasoline ignition map is compared vis-à-vis recalibrated M85 ignition map for varying engine speed and three representative throttle opening positions at 0, 40% and 80%. Fig. 5(a) and 5(b) show the ignition map for gasoline and M85 respectively. Fig. 5(c) compares the spark timing of stock gasoline-fuelled vehicle vis-à-vis recalibrated M85-fuelled vehicle at varying engine speeds for three different throttle positions (0, 40% and 80%).



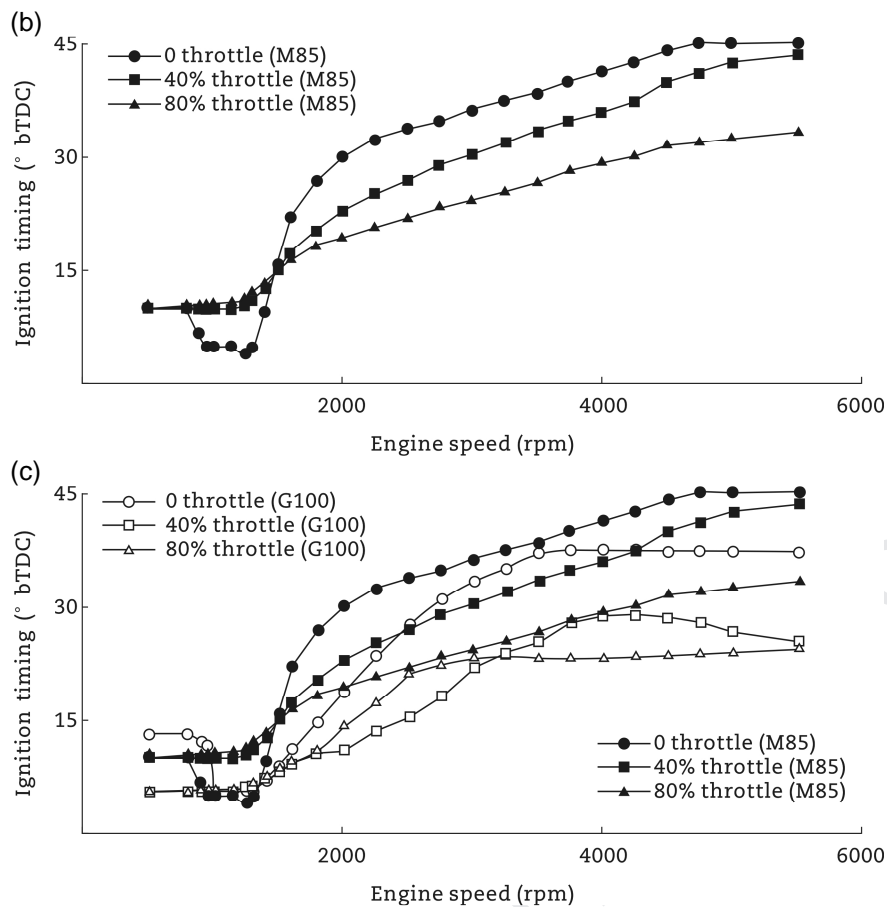


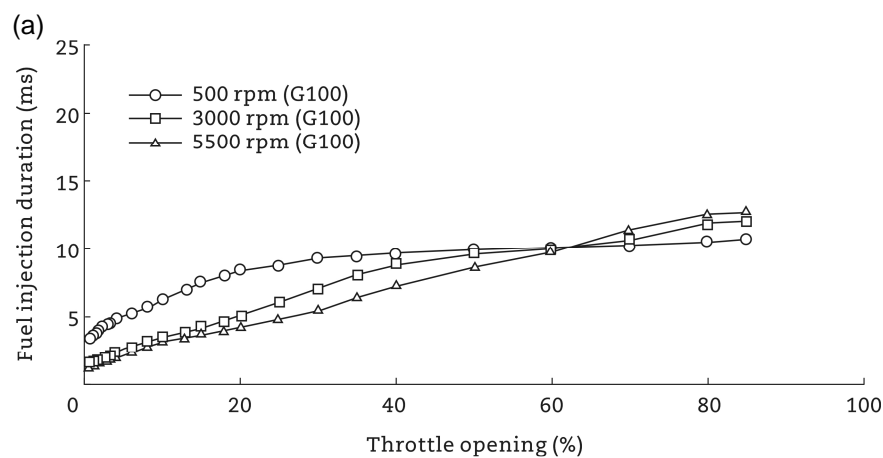
Fig. 5 Comparison of base gasoline ignition map vis-à-vis recalibrated M85 ignition map. (a) G100. (b) M85. (c) G100 vs. M85.

It can be observed that at engine speed around 500 rpm and throttle below 2%, ignition timing was significantly advanced compared to nearby region. This was because at that engine speed, the engine was in the starting zone. At low engine speed and almost closed throttle position, fuel energy provided to the engine is very low. Hence, in order to sustain the combustion and successfully start the engine, spark advance had to keep higher in order to extract maximum power output from the engine under given conditions. Another important trend seen for engine speed ranging from 500 to 1050 rpm was that first the spark advance decreased and then from 1050 to 1300 rpm, it remained constant instead of increasing with the engine speed. This is known as “bucket strategy”. This strategy is used to maintain the engine idling speed at around 1050 rpm. If during idling, the engine speed tends to decrease, higher spark advance at lower engine speed provides a power boost and increases the engine speed to the idling speed. And if the engine tends to go beyond 1050 rpm during idling, it does not get any boost since there is no change in spark timing or fuel injection and engine speed is therefore maintained at around 1050 rpm.

It was observed that spark timing was advanced for higher in case of M85 across entire range. Methanol has higher octane rating of 109% as compared to 95% of gasoline. This allows M85 to burn more efficiently with higher spark advance without possibility of knocking. M85-fuelled vehicle can therefore go up to 45° bTDC spark advance compared to maximum spark advance of 37° bTDC in case of gasoline. It was also observed that as the engine speed increased, difference between spark advance for M85 and gasoline also increased. At higher engine speeds, engine temperature increased. In case of gasoline, this led to a serious problem, resulting in auto-ignition encountered by the hot spots and thus engine starts knocking. However, in case of M85, one can go to significantly higher spark advance due to its higher-octane rating and intake charge cooling characteristics of methanol because of higher latent heat of vaporization also assisted in suppressing the engine knocking.

3.2 Comparison of gasoline fuel map vis-à-vis M85 fuel map

Fig. 6 compares the injector opening duration in milliseconds of the stock gasoline-fuelled vehicle vis-à-vis recalibrated M85-fuelled vehicle at varying throttle position for three different representative engine speeds (500, 3000 and 5500 rpm). The fuel quantity injected for M85 is roughly twice that of gasoline, because methanol has approximately half the energy density as compared to gasoline. It was also observed that at around 60% throttle opening, the injection opening duration graphs intersected and not increased significantly with increasing throttle. This was because the intake air flow became saturated beyond this point and no significant change took place until the vehicle speed increased simultaneously.



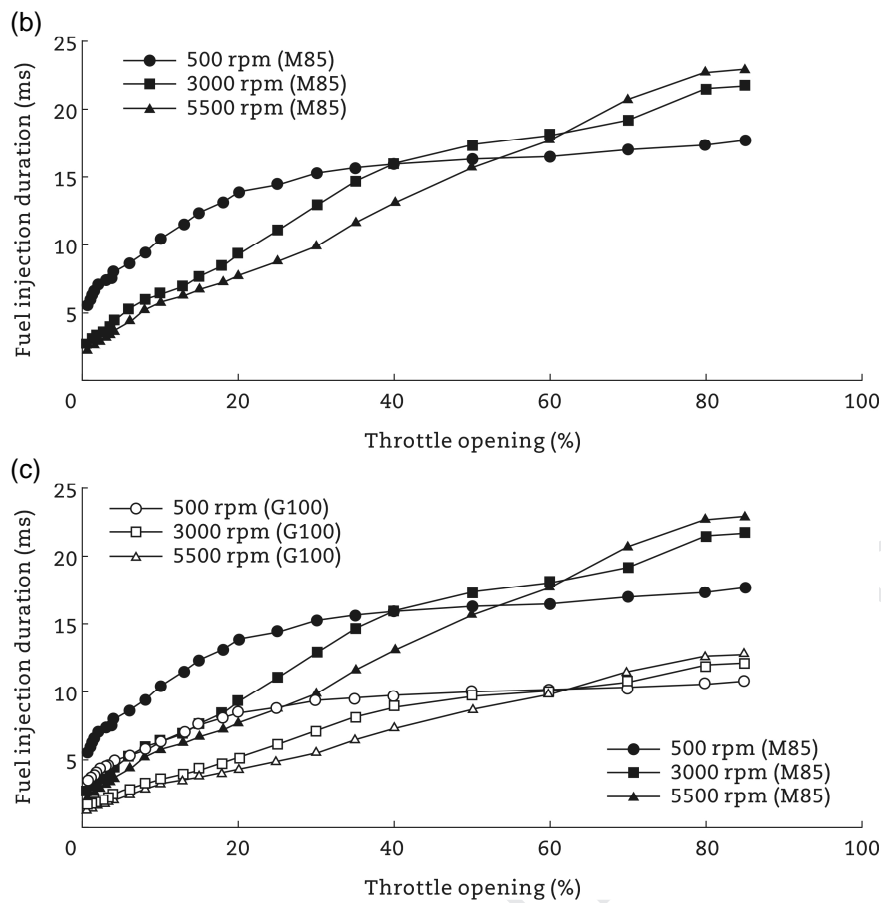


Fig. 6 Comparison of the base gasoline fuel map vis-à-vis recalibrated M85 fuel map. (a) G100. (b) M85.
(c) G100 vs. M85.

3.3 Comparative vehicle performance analysis of gasoline vis-à-vis M85-fuelled vehicle

Once the ECU was recalibrated for M85 according to industry standards, the performance of modified vehicle was compared vis-à-vis stock gasoline vehicle to validate the M85 recalibration settings. For this test, both the vehicles were operated on a chassis dynamometer under simulated road driving conditions. Following industry standard performance tests were performed on the chassis dynamometer for comparing them: (i) maximum speed, (ii) power at wheels, (iii) acceleration-speed-based, (iv) acceleration-distance-based, and (v) overtaking acceleration.

3.3.1 Maximum vehicle speed and power at wheels

As seen in Fig. 7, M85-fuelled vehicle generated 5.8% higher power output as compared to gasoline-fuelled vehicle. M85-fuelled vehicle reached 2.2% higher maximum speed as compared to gasoline-fuelled vehicle (Fig. 8).

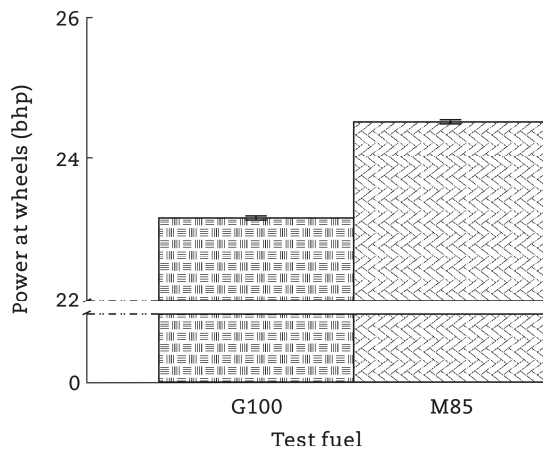


Fig. 7 Maximum power at wheels for gasoline vs. M85 at wide open throttle (WOT).

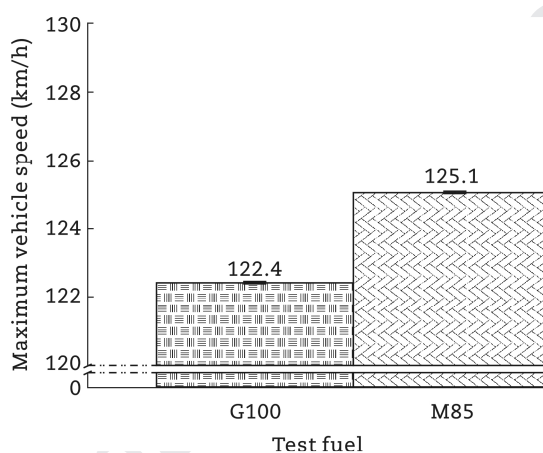


Fig. 8 Maximum vehicle speed achieved for gasoline vs. M85 at wide open throttle (WOT).

There are many reasons for this. First, octane rating of methanol (109%) is significantly higher than baseline gasoline (95%), which allows M85-fuelled motorcycle to operate with high spark advance compared to gasoline-fuelled vehicle. This produced higher in-cylinder peak pressure thereby higher power at the wheel. Second, the laminar flame speed of methanol is significantly higher compared to the baseline gasoline. Higher laminar flame speed increased BTE of the engine by attaining more complete combustion relatively earlier, which also decreased heat losses from the engine cylinder. Third, M85 has about 44% fuel oxygen content as compared to gasoline. This improved the combustion and resulted in improved BTE. Fourth, the LHV of methanol (1089 kJ/kg) is about 3 times higher compared to the baseline gasoline (375 kJ/kg). Therefore, methanol absorbed more heat from the in-cylinder contents during its vaporization in the compression stroke. This cooled down the intake charge and increased the density of combustible mixture, which in turn increased the volumetric efficiency of the engine. This also decreased the required work for compressing the fuel-air mixture,

thus improving overall power output for M85-fuelled vehicle.

3.3.2 Acceleration test

Acceleration is one of the most important performance characteristics of any vehicle. It is a more important parameter compared to maximum vehicle speed or maximum power because good acceleration enables the vehicle to gain speed quickly from standstill condition and is appealing to the customers. Better acceleration provides better vehicle drivability due to quicker throttle response. Vehicles with poor acceleration feel sluggish and unpleasant to drive. There are two types of acceleration tests performed in automotive industry: (i) speed-based acceleration test, and (ii) distance-based acceleration test. Both the tests were performed and compared for the two vehicles.

(1) Speed-based acceleration test

In speed-based acceleration test, driver starts the vehicle from standstill condition and tries to achieve the maximum possible speed in minimum possible time on a chassis dynamometer. Dynamometer controller logs the time stamp from idling to maximum speed achieved at an interval of 10 km/h. Vehicle taking less time to reach a particular speed is considered to have better acceleration. As seen in Fig. 9, vehicle acceleration can be divided into two zones, based on the time taken by gasoline and M85-fuelled vehicles to achieve a particular speed: low-speed zone (0–80 km/h) and high speed zone (81–120 km/h).

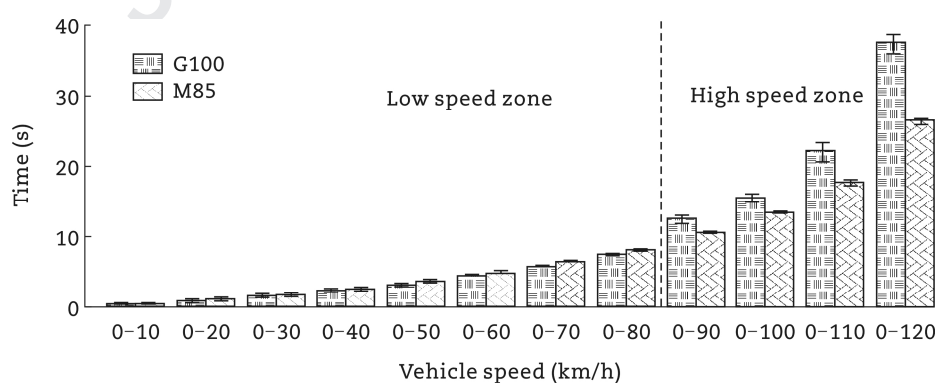


Fig. 9 Speed-based acceleration test for M85 and gasoline two-wheeler on a chassis dynamometer.

Low speed zone. In low speed zone, the acceleration for M85-fuelled vehicle was slightly lower than gasoline-fuelled vehicle. At low vehicle speed, engine has relatively lower temperature. Since LHV of methanol is three times higher than gasoline, M85 was not adequately vaporized hence remains

unburnt partially before leaving the cylinder. Thus, at low temperature, M85-fuelled engine resulted in incomplete combustion and power output from M85-fuelled engine was lower than expected. Also, in case of M85, almost twice fuel quantity was injected compared to gasoline because of its lower calorific value. Hence, M85-fuelled engine required more heat to vaporize the fuel entirely and form a combustible charge.

High speed zone. In high speed zone, acceleration for M85-fuelled vehicle was superior to gasoline. Comparison of acceleration trends of low and high speed zones clearly showed that time required for acceleration of both gasoline and M85-fuelled vehicles increased with increasing engine speed, however relative increase of time for gasoline-fuelled vehicle was relatively higher compared to M85-fuelled vehicle at this critical speed. As the vehicle speed increased, engine temperature also increased. Because of increased engine temperature methanol in the fuel adequately vaporized, leading to more complete combustion of M85. At higher engine speed, dominant effect of fuel-bound oxygen in methanol might be a major reason for superior acceleration of M85 compared to gasoline (Han et al., 2019).

(2) Distance-based acceleration test

Distance-based acceleration test is frequently used in automotive industry for performance benchmarking. This test is quite similar to speed-based acceleration test, however, instead of logging the target speed time stamp, chassis dynamometer logs the distance time step from 0 to 400 m at an interval of 100 m. This test reveals how fast the test vehicle covers a particular distance from the standstill. Fig. 10 shows that time taken by M85-fuelled vehicle was 4% less than base gasoline-fuelled vehicle. Hence, M85-fuelled vehicle gives better ride feeling compared to gasoline-fuelled motorcycle, especially when throttle is pulled suddenly.

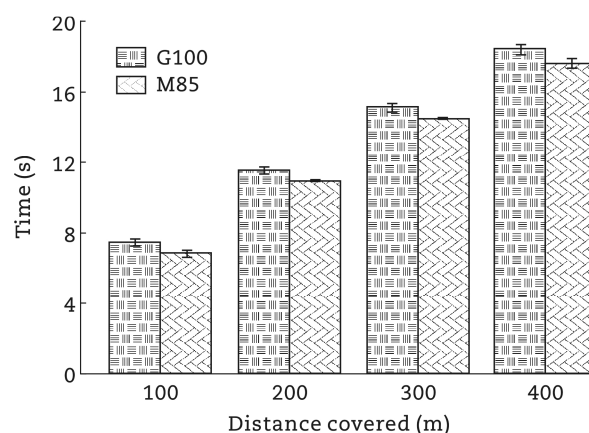


Fig. 10 Distance-based acceleration test for M85 and gasoline two-wheeler on a chassis dynamometer.

3.3.3 Overtaking acceleration

Overtaking acceleration is also one of the important performance parameters, which is used in automotive industry for benchmarking the drivability of a test vehicle. This test is similar to speed-based acceleration test, but instead of starting test vehicle from standstill to maximum speed, vehicle is accelerated from a constant non-zero speed to a predefined higher speed in a fixed gear. This test simulates the real-life highway riding condition, in which rider needs to overtake vehicle in front of him/her. In such scenarios, there is not enough time to switch the gears and vehicle needs to be accelerated from the gear in which it is already running.

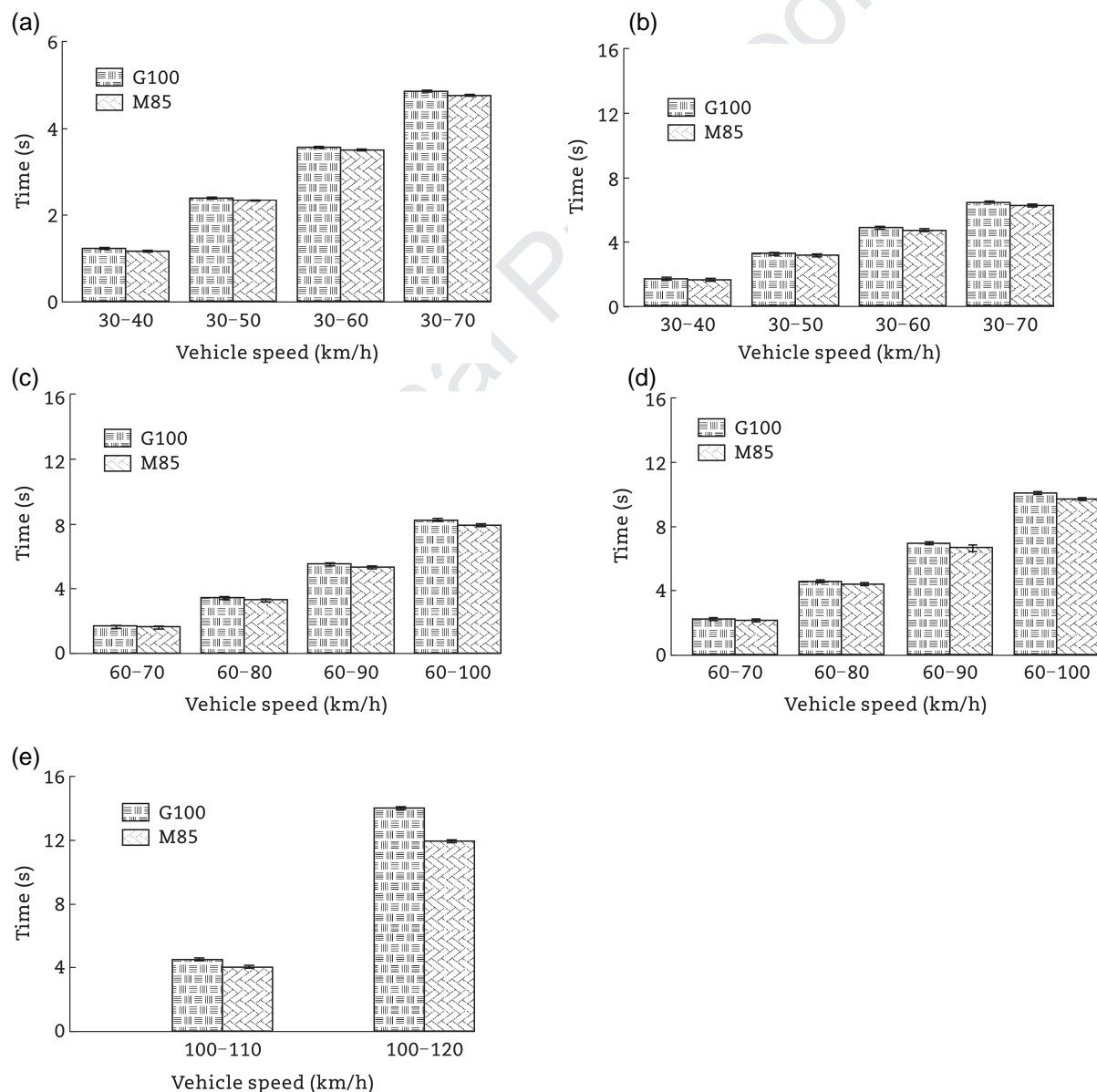


Fig. 11 Overtaking acceleration test for M85 and gasoline two-wheeler on a chassis dynamometer. (a) 3rd gear. (b) 4th gear (30–70 km/h). (c) 4th gear (60–100 km/h). (d) 5th gear (60–100 km/h). (e) 5th gear (100–120 km/h).

Fig. 11 compares the overtaking acceleration of gasoline-fuelled vehicle vis-à-vis M85-fuelled vehicle for 3rd, 4th, and 5th gear. It can be seen that in all cases the acceleration of M85-fuelled vehicle is slightly better compared to the baseline gasoline-fuelled vehicle. Even at lower speed, vehicle acceleration was superior for M85 because the vehicle was already running at some constant speed, thus the engine temperature was sufficiently high to allow complete vaporization of methanol in the test fuel, leading to more complete combustion of M85.

3.4 Comparative tailpipe emissions from gasoline and M85-fuelled two-wheelers

Tailpipe emissions were measured using a raw exhaust gas emission analyzer. The vehicle was operated on the chassis dynamometer from standstill condition (idling) to 120 km/h and emissions were recorded in steps of every 10 km/h. All regulated emissions such as CO, NO_x and HC were logged as raw emissions and were reported for both fuels for comparative analysis. To support the CO and HC emissions, lambda measured at tailpipe is presented Fig. 12.

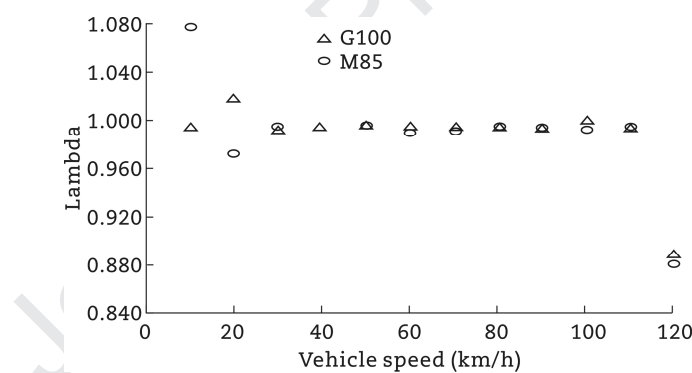


Fig. 12 Lambda with regard to vehicle speed for gasoline and M85.

3.4.1 Carbon monoxide (CO)

Fig. 13 shows the effect of vehicle speed and test fuel on CO emission. CO is a toxic by-product forming due to incomplete combustion of hydrocarbon fuels (De et al., 2019). CO emission decreased with increasing vehicle speed, reached a minimum and then increased again. At low vehicle speed and low engine load, the peak in-cylinder temperature was very low, which led to incomplete oxidation of CO to CO₂. At very high vehicle speed, CO to CO₂ was hampered by richer fuel-air mixture, which led to insufficient oxygen available for CO oxidation (Heywood, 1988). These results are similar to the previous studies reported in literature (Li et al., 2015).

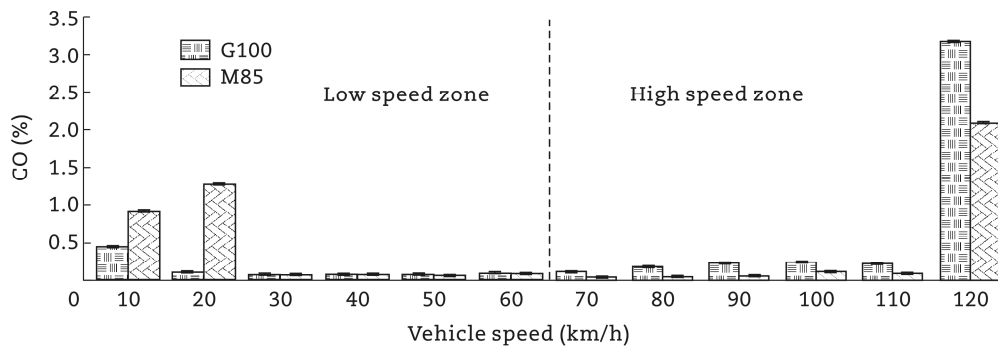


Fig. 13 CO emissions with regard to vehicle speed for gasoline and M85.

In the low vehicle speed region (0–60 km/h), CO emission from M85 was observed to be slightly higher compared to gasoline. At low vehicle speed, engine operated at relatively lower peak temperature. At low in-cylinder temperature, M85 was not completely vaporized due to its relatively higher LHV. Hence, M85-fuelled engine resulted in incomplete combustion. However, in the high vehicle speed region (61–120 km/h), CO emission was relatively lower for M85-fuelled vehicle compared to base gasoline vehicle. As the engine in-cylinder temperature increased, methanol presents the test fuel was adequately vaporized. Also, presence of · OH radicals in methanol helped in more efficient oxidation of CO to CO₂ as compared to gasoline.

3.4.2 Oxides of nitrogen (NO_x)

Fig. 14 shows the effect of vehicle speed and test fuels on NO_x emission. NO_x formation takes place due to oxidation of atmospheric nitrogen at high in-cylinder temperature in the engine. It was observed that NO_x emission increased with increasing vehicle speed. At high vehicle speed, the fuel injected into the engine was also higher, which led to relatively higher peak in-cylinder pressure and temperature, resulting in higher NO_x formation and emission. As observed in Fig. 14, M85-fuelled vehicle emitted relatively higher NO_x compared to baseline gasoline-fuelled vehicle. Higher octane rating of methanol allowed combustion of leaner fuel-air mixture at relatively higher in-cylinder temperature without knocking. This led to higher NO_x emission from M85-fuelled vehicle. Superior fuel efficiency resulted in higher NO_x emission in recalibrated M85-fuelled vehicle. However, NO_x emissions can be effectively taken care of by selecting an effective three-way catalytic converter, specifically designed for methanol.

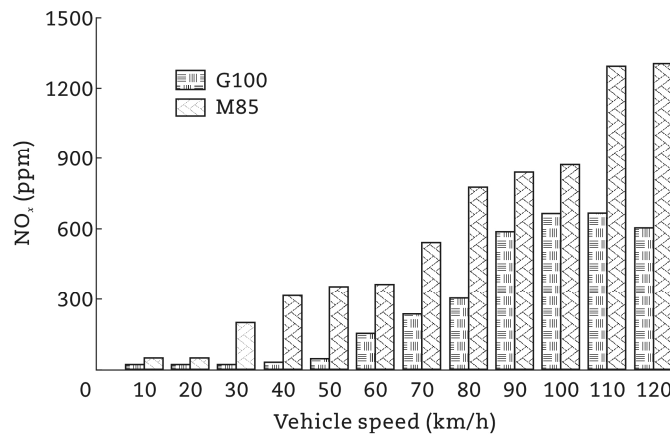


Fig. 14 NO_x emission with regard to vehicle speed for gasoline and M85.

3.4.3 Hydrocarbons (HC)

Fig. 15 shows the effect of vehicle speed and test fuels on tailpipe HC emissions for M85 and gasoline-fuelled two-wheelers. HC emissions are a consequence of incomplete combustion of fuel. It was observed that as the vehicle speed increased, HC emissions decreased. At lower vehicle speed (0–70 km/h) and load, the combustion chamber temperature was relatively lower and incomplete vaporization and combustion of test fuel took place under these conditions. However, as the combustion chamber temperature increased, HC emissions reduced due to relatively more complete combustion. Another important observation was that in the low vehicle speed region, HC emissions were higher from M85-fuelled vehicle compared to base gasoline-fuelled vehicle. At low vehicle speeds, engine operates at relatively lower in-cylinder temperature, wherein M85 is not fully vaporized due to its higher LHV. M85-fuelled engine therefore undergoes incomplete combustion, leading to higher HC tailpipe emissions. However, as the engine temperature increased with increasing vehicle speed, methanol vaporized more effectively, leading to comparable HC emissions from M85 and gasoline-fuelled vehicles.

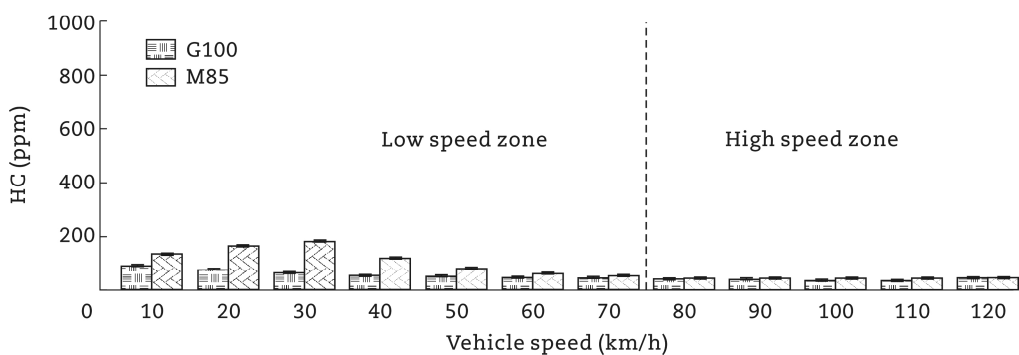


Fig. 15 HC emissions with regard to vehicle speed for gasoline and M85.

4 Conclusions

In this study, a naturally aspirated 500 cc gasoline engine was modified into a M85-fuelled engine for a two-wheeler prototype. This was achieved by replacing the stock gasoline ECU with an open ECU and recalibrating it for M85. Results showed that the modified M85-fuelled engine can be operated with more advanced spark timings without knocking. M85-fuelled vehicle required about 1.85 times higher fuel quantity injected per cycle for similar power output as gasoline-fuelled vehicle. M85-fuelled vehicle produced relatively higher power output and top speed compared to equivalent gasoline-fuelled vehicle. At low vehicle speeds, accelerations of stock gasoline-fuelled vehicle and modified M85-fuelled vehicle were comparable. However, at higher vehicle speeds, M85-fuelled vehicle showed higher acceleration compared to stock gasoline-fuelled motorcycle. Overtaking acceleration for M85-fuelled motorcycle was also superior compared to stock gasoline-fuelled motorcycle, which provided better rider feel and superior throttle response. Emission results exhibited that M85-fuelled vehicle emitted relatively higher HC and CO emissions compared to stock gasoline-fuelled motorcycle, which reduced at higher engine speeds. Relatively higher NO_x emissions from M85-fuelled vehicle compared to stock gasoline-fuelled motorcycle was an important finding of this study.

Conflict of interest

The authors do not have any conflict of interest with other entities or researchers.

Acknowledgments

The authors would like to acknowledge the Royal Enfield (Mr. Bala Kishore and Mr. Amit Kaul) for their continued collaboration and support in this project.

Appendix

A.1. Generate base fuel map and ignition map for gasoline by reverse engineering

For this experimental study, the engine was operated at constant engine speeds using an engine dynamometer and throttle opening was varied from 0 to 85% at pre-defined intervals. The spark plug and fuel injector signals originating from ECU were tapped using current clamps.

A.1.1 Base ignition map for gasoline

The base ignition timing map hold the spark timing values used with the lowest octane fuel for the engine. This was the most retarded timing for running the engine under normal circumstances. For obtaining the gasoline base ignition map, the engine was operated at constant engine speeds at 500, 800, 900, 950, 1000, 1150, 1250, 1300, 1400, 1500, 1600, 1800, 2000, 2500, 2750, 3000, 3250, 3500, 3750, 4000, 4250, 4500, 4750, 5000 and 5500 rpm, at different throttle openings ranging from 0 to 80% (0, 0.7%, 1.3%, 2%, 3%, 5%, 6%, 10%, 13%, 15%, 20%, 25%, 30%, 35%, 40%, 45%, 50%, 55%, 60%, 65%, 70%, 75% and 80%) and varying spark timing before top dead centre (bTDC) was logged on to the combustion analyzer by tapping the spark plug input signal. Base ignition map (3-D) thus generated is shown in Fig. A1.

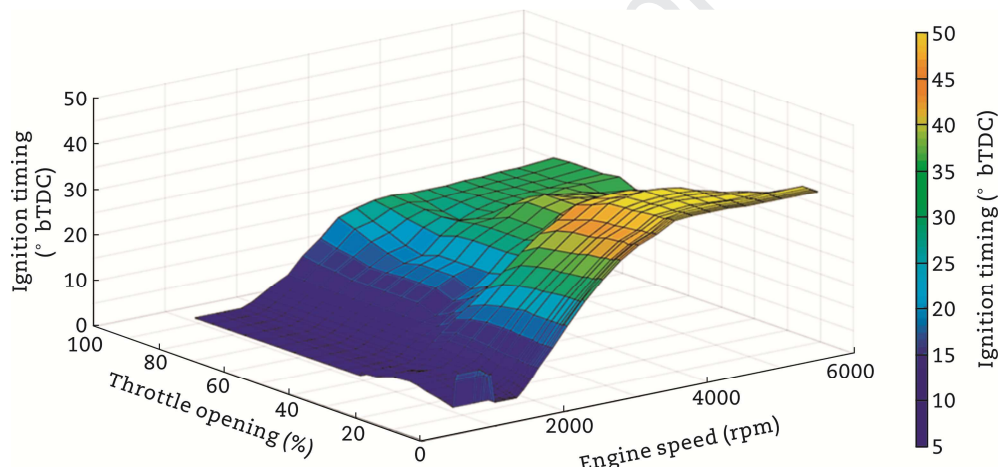


Fig. A1 Baseline map for fuel ignition timing

As seen in Fig. A1, when engine speed increased, ignition advance also increased. And as engine load increased, ignition timing got retard. The highest ignition advance was used at high engine speeds and low loads, while the least advance was used at high loads and low engine speeds. Also, the ignition timing flattens off at high engine speeds. This was because at high engine speeds, the tendency of knocking increased and ECU used “safe” timing values in that region.

A.1.2 Base fuel map for gasoline

Base gasoline holds the value of injector open time in milliseconds for a particular engine speed and throttle opening. The process of generating fuel map was similar to that of generating ignition map. For obtaining the base gasoline fuel map, the engine was operated at constant engine speeds at 500, 800,

900, 950, 1000, 1100, 1200, 1300, 1400, 1500, 1750, 2000, 2250, 2500, 2750, 3000, 3250, 3500, 3750, 4000, 4250, 4500, 4750, 5000, 5250 and 5500 rpm, at different throttle opening ranging from 0 to 85% (0.7%, 1.0%, 1.3%, 1.7%, 2%, 2.7%, 3.3%, 4%, 6%, 8%, 10%, 13%, 15%, 18%, 20%, 25%, 30%, 35%, 40%, 50%, 60%, 70%, 80% and 85%). Injector open time (ms) was logged on to the combustion analyzer by tapping the fuel injector input signal. The throttle opening values in the range of 0 to 10% were more kept closely spaced compared to rest of the table. This was because the fuel quantity injected into the engine cylinder was directly proportional to its power output. Thus, finer fuel calibration at lower throttle opening resulted in better throttle response, when vehicle was started from standstill. The 3-D graph for base gasoline ignition map generated in this experiment is shown in Fig. A2.

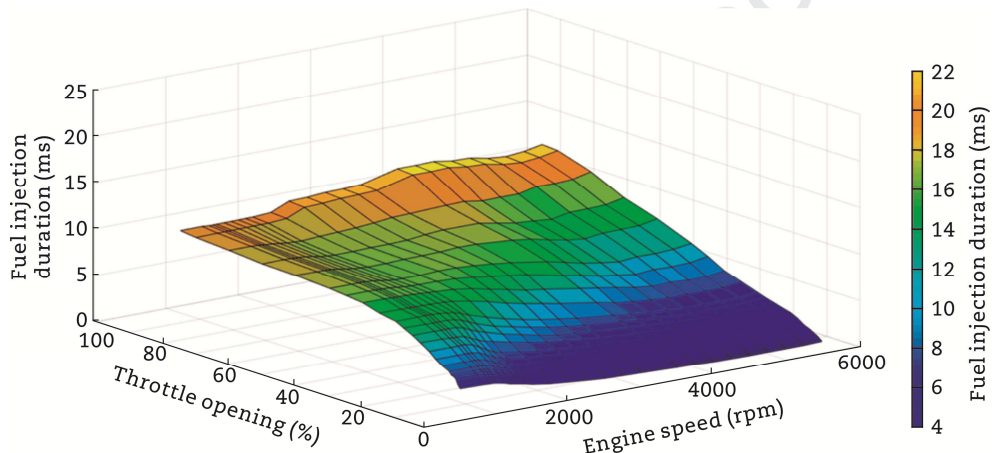


Fig. A2 Baseline map for fuel injection quantity.

It was observed that as the throttle increased, the fuel injected into the engine cylinder also increased, because with increasing throttle, more power output was expected, hence more fuel was required to sustain increased load demand. It was also observed that fuel injection duration did not increase significantly with increasing engine speed. This was because the fuel table reflects the fuel injected per engine cycle and not per unit time. The total fuel consumed per unit time increased with increasing engine speed, however, for a single engine cycle, it did not increase significantly with increasing engine speed.

A.2. Fuel and ignition map recalibration for M85

Using the base gasoline maps as starting point, crude maps for M85 were estimated. Using these crude maps, ECU was calibrated and fine-tuned for M85 on the chassis dynamometer.

A.2.1 Ignition map for M85

Once the default tables are crudely developed, the map was recalibrated to freeze the ignition timing with the highest engine torque output. The final ignition map obtained for M85 is shown in Fig. A3.

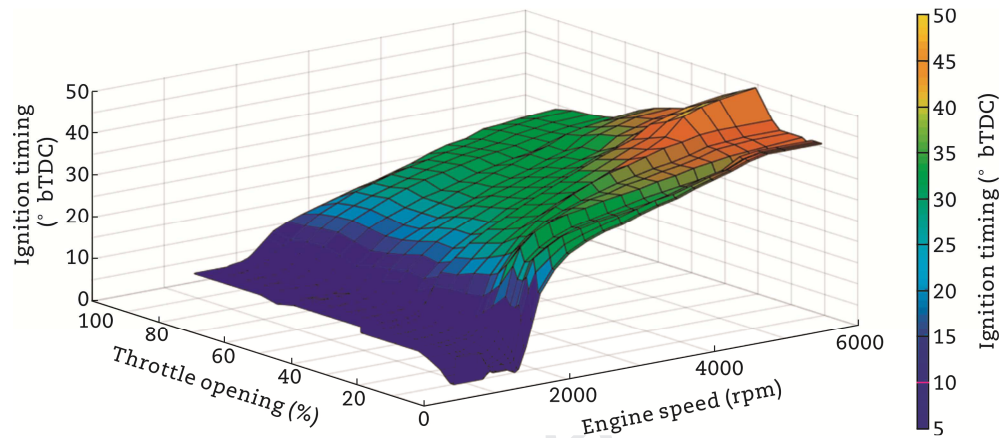


Fig. A3 Ignition map for M85.

It can be observed that M85 has relatively higher spark advance angle as compared to gasoline for most points. Methanol has higher octane rating of 109% compared to 95% for gasoline. This allows M85 to burn more efficiently with higher spark advance compared to baseline gasoline without knocking, which is reflected clearly in Fig. A3.

A.2.2 Fuel map for M85

The fuel maps for M85 were crudely estimated from the gasoline base fuel maps by using concept of energy balance. Once the crude base fuel maps for M85 were generated, next step was the fine-tuning of fuel maps for M85. For a particular engine speed and throttle input given by the rider, the engine should be able to provide the same power output for both gasoline and M85. This can be achieved by multiplying the injector open time for gasoline by a factor of 1.85 (using the concept of energy balance). Once crude fuel map for M85 were generated, ECU was fine-tuned for maximum torque output for each engine speed and throttle position combination in the recalibrated fuel map for M85. The final fuel map generated for M85 is shown in Fig. A4.

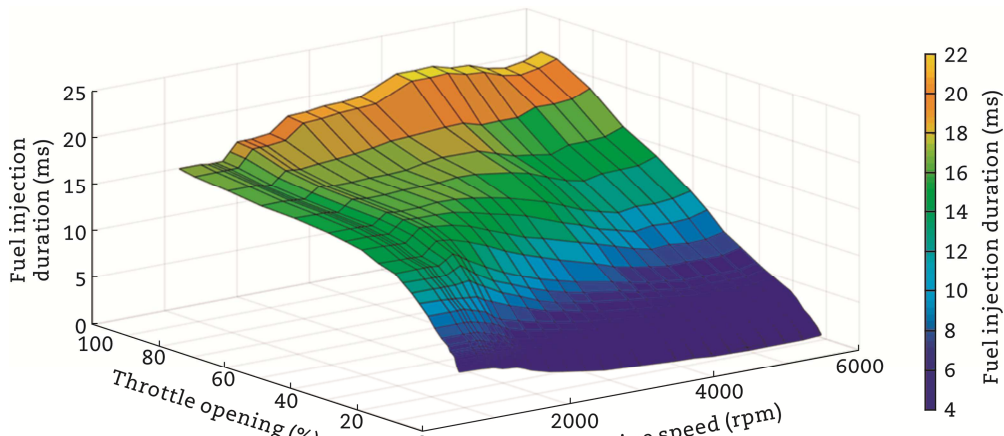


Fig. A4 Fuel map for M85.

References

- Agarwal, A.K., 2007. Biofuels (alcohols and biodiesel) applications as fuels for internal combustion engines. *Progress in Energy and Combustion Science* 33(3), 233-271.
- Agarwal, A.K., Karare, H., Dhar, A., 2014. Combustion, performance, emissions and particulate characterization of a methanol–gasoline blend (gasohol) fuelled medium duty spark ignition transportation engine. *Fuel Processing Technology* 121, 16-24.
- Agarwal, A.K., Sharma, N., Singh, A.P., et al., 2019. Adaptation of methanol–dodecanol–diesel blend in diesel genset engine. *Journal of Energy Resources Technology* 141(10), 102203.
- Agarwal, T., Singh, A.P., Agarwal, A.K., 2020. Development of methanol fuelled two-wheeler for sustainable mobility. In: *Advanced Combustion Techniques and Engine Technologies for the Automotive Sector*. Springer, New York, pp. 9-36.
- Anderson, J.E., Kramer, U., Mueller, S.A., et al., 2010. Octane numbers of ethanol- and methanol–gasoline blends estimated from molar concentrations. *Energy & Fuels* 24(12), 6576-6585.
- Chen, Y., Ma, J., Han, B., et al., 2018. Emissions of automobiles fueled with alternative fuels based on engine technology: a review. *Journal of Traffic and Transportation Engineering (English Edition)*

- 5(4), 318-334.
- Chen, Z., Chen, H., Wang, L., et al., 2020. Parametric study on effects of excess air/fuel ratio, spark timing, and methanol injection timing on combustion characteristics and performance of natural gas/methanol dual-fuel engine at low loads. *Energy Conversion and Management* 210, 112742.
- Costagliola, M.A., Prati, M.V., Murena, F., 2016. Bioethanol/gasoline blends for fuelling conventional and hybrid scooter. Regulated and unregulated exhaust emissions. *Atmospheric Environment* 132, 133-140.
- Dey, S., Dhal, G.C., Mohan, D., et al., 2019. Application of hopcalite catalyst for controlling carbon monoxide emission at cold-start emission conditions. *Journal of Traffic and Transportation Engineering (English Edition)* 6(5), 419-440.
- Dhaliwal, B., Yi, N., Checkel, D., 2000. Emissions Effects of Alternative Fuels in Light-duty and Heavy-duty Vehicles. *SAE Technical Paper 2000-01-0692*. SAE, Detroit.
- Geng, L., Wang, Y., Wang, Y., et al., 2018. Effect of the injection pressure and orifice diameter on the spray characteristics of biodiesel. *Journal of Traffic and Transportation Engineering (English Edition)*, doi:10.1016/j.jtte.2018.12.004
- Gong, C., Li, J., Li, J., et al., 2011. Effects of ambient temperature on firing behavior and unregulated emissions of spark-ignition methanol and liquefied petroleum gas/methanol engines during cold start. *Fuel* 90(1), 19-25.
- Han, Z., Li, B., Tian, W., et al., 2019. Influence of coupling action of oxygenated fuel and gas circuit oxygen on hydrocarbons formation in diesel engine. *Energy* 173, 196-206.
- Heywood, J.B., 1988. Internal Combustion Engine Fundamentals. McGraw-Hill Book Company, New York.
- Iliev, S., 2018. Comparison of ethanol and methanol blending with gasoline using engine simulation. In: Al Qubeissi, M. (Ed.), *Biofuels—Challenges and Opportunities*. IntechOpen. London.
- Latey, A.A., Bhatti, T.S., Das, L.M., et al., 2005. Methanol Blended Fuel Investigations on an Injected Single Cylinder Spark Ignition Engine. *SAE Technical Paper 2005-26-031*. SAE, Detroit.
- Li, L., Ge, Y., Wang, M., Li, J., et al., 2015. Effect of gasoline/methanol blends on motorcycle emissions: exhaust and evaporative emissions. *Atmospheric Environment* 102, 79-85.
- Liao, S.Y., Jiang, D.M., Cheng, Q., et al., 2005. Investigation of the cold start combustion characteristics of ethanol–gasoline blends in a constant-volume chamber. *Energy & Fuels* 19, 813-819.

- Nesamani, K.S., Saphores, J., McNally, M.G., et al., 2017. Estimating impacts of emission specific characteristics on vehicle operation for quantifying air pollutant emissions and energy use. *Journal of Traffic and Transportation Engineering (English Edition)* 4(3), 215-229.
- Nichols, R.J., 2003. The methanol story: a sustainable fuel for the future. *Journal of Scientific & Industrial Research* 62(1), 97–105.
- No, S.Y., 2017. Application of straight vegetable oil from triglyceride based biomass to IC engines—a review. *Renewable and Sustainable Energy Reviews* 69, 80-97.
- Pal, A., Agarwal, A.K., 2015. Comparative study of laser ignition and conventional electrical spark ignition systems in a hydrogen fuelled engine. *International Journal of Hydrogen Energy* 40(5), 2386-2395.
- Patel, C., Tiwari, N., Agarwal, A.K., 2019. Experimental investigations of Soyabean and Rapeseed SVO and biodiesels on engine noise, vibrations, and engine characteristics. *Fuel* 238, 86-97.
- Paramasivam, S., Subramanian, K.A., Mathai, R., 2018. Driving cycle performance and emission analysis of a motorcycle with gasoline and E20 fuels. In: 11th International Symposium on Fuels and Lubricants (ISFL), New Delhi, 2018.
- Paramasivam, S., Subramanian, K.A., Mathai, R., 2019. Comparative studies on combustion, performance and emission characteristics of a two-wheeler with gasoline and 30% ethanol-gasoline blend using chassis dynamometer. *Applied Thermal Engineering* 146, 726-737.
- Paramasivam, S., Subramanian, K.A., Mathai, R., 2020. Experimental study on unregulated emission characteristics of a two-wheeler with ethanol-gasoline blends (E0 to E50). *Fuel* 262, 116504.
- Singh, A.P., Jain, A., Agarwal, A.K., 2017a. Fuel injection strategy for PCCI engine fueled by mineral diesel and biodiesel blends. *Energy & Fuels* 31(8), 8594-8607.
- Singh, A.P., Pal, A., Gupta, N.K., et al., 2017b. Particulate emissions from laser ignited and spark ignited hydrogen fueled engines. *International Journal of Hydrogen Energy* 42(24), 15956-15965.
- Singh, S.B., Dhar, A., Agarwal, A.K., 2015. Technical feasibility study of butanol–gasoline blends for powering medium-duty transportation spark ignition engine. *Renewable Energy* 76, 706-716.
- Siwale, L., Kristóf, L., Bereczky, A., et al., 2014. Performance, combustion and emission characteristics of n-butanol additive in methanol–gasoline blend fired in a naturally-aspirated spark ignition engine. *Fuel Processing Technology* 118, 318-326.
- Smil, V., 2017. *Energy Transitions: Global and National Perspectives*. Praeger, San Matoe.

- Verhelst, S., Turner, J.W.G., Sileghem, L., et al., 2019. Methanol as a fuel for internal combustion engines. *Progress in Energy and Combustion Science* 70, 43-88.
- Wei, Y., Liu, S., Li, H., et al., 2008. Effects of methanol/gasoline blends on a spark ignition engine performance and emissions. *Energy & Fuels* 22(2), 1254-1259.
- Yang, H., Liu, T., Chang, C., et al., 2012. Effects of ethanol-blended gasoline on emissions of regulated air pollutants and carbonyls from motorcycles. *Applied Energy* 89(1), 281-286.
- Yao, Y., Chang, Y., Huang, R., et al., 2018. Environmental implications of the methanol economy in China: well-to-wheel comparison of energy and environmental emissions for different methanol fuel production pathways. *Journal of Cleaner Production* 172, 1381-1390.



Tushar Agarwal is a mechanical engineer. He graduated from Indian Institute of Technology Kanpur, with bachelor's and master's degrees in mechanical engineering from Engine Research Laboratory of IIT Kanpur, under the supervision of Prof. Avinash Kumar Agarwal. Tushar Agarwal worked on the development of methanol fuel motorcycle for his master's degree, for which he was awarded with "ISEES Best Master's Thesis Award-2020" by International Society of Energy, Environment and Sustainability (ISEES). Tushar is currently working as Sr. product manager at Nocca Robotics Pvt. Ltd. He was a recipient of SY Jakatdar Scholarship for excellence in automotive engineering and has authored one book chapter. He has been part of many science and technology societies of IIT Kanpur namely electronics club, Boeing abhasynt, robotics club and IITK Motorsports.



Dr. Akhilendra Pratap Singh is working at IIT Kanpur. He received his master's degree and PhD in mechanical engineering from Indian Institute of Technology Kanpur in 2010 and 2016 respectively. His areas of research include advanced low temperature combustion; optical diagnostics with special reference to engine endoscopy and PIV; combustion diagnostics; engine emissions measurement; particulate characterization and their control; and alternative fuels. Dr. Singh has edited 10 books and authored 25 book chapters, 45 research articles in international journals and conferences. He has been awarded with "ISEES Best PhD Thesis Award" (2017), "SERB Indo-US Postdoctoral Fellowship" (2017), "IEI Young Engineer Award" (2017) and "ISEES Young Scientist Award" (2018). He is a member of numerous professional societies, including SAE, ASME, and ISEES.



Prof. Avinash Kumar Agarwal is serving as SBI Endowed Chair Professor at Department of Mechanical Engineering, Indian Institute of Technology Kanpur. He works in the areas of IC engines, combustion, conventional fuels, alternative fuels, fuel sprays, optical diagnostics, laser ignition, HCCI, particulate and emission control, and large bore engines. Prof. Agarwal has published over 280 peer reviewed international journal and conference papers, 35 edited books, 63 books chapters and has more than 9600 Scopus and more than 14500 Google scholar citations. He is associate principle editor of "Fuel". For his outstanding contributions, Prof. Agarwal is conferred upon J C Bose National Fellowship (2019) by SERB, Clarivate Analytics India Citation Award-2017 in Engineering and Technology, Prestigious Shanti Swarup Bhatnagar Prize (2016) in Engineering Sciences, among many awards. He is an elected Fellow of Society of Automotive Engineers International, USA, American Society of Mechanical Engineers, Indian National Academy of Engineering, International Society for Energy, Environment and Sustainability, Royal Society of Chemistry, National Academy of Science Allahabad and American Association for Advancement in Science.